

EVALUATION OF TRANSONIC BUFFETING ONSET BOUNDARY ESTIMATED BY TRAILING EDGE PRESSURE DIVERGENCE AND RMS DATA OF WING VIBRATION

Rodrigo Sorbilli C. de Sousa^{*}, Roberto da Motta Girardi^{**} Roberto Gil Annes da Silva^{**}
^{*}EMBRAER, ^{**}Instituto Tecnológico de Aeronautica

Keywords: buffeting onset, wind tunnel, transonic, wing pressure, strain gauge

Abstract

An evaluation of the transonic buffeting onset boundary estimated by trailing edge pressure and RMS (root mean square) data of wing root strain is presented. The analysis is based on wind tunnel data of two modern transonic aircraft. The results obtained with the pressure and wing vibration data are compared to a steady aerodynamics coefficient methodology that was evaluated with flight test results. The evaluation concludes that strain gauge data provides a mean of quantifying the buffeting onset magnitude that can be correlated to flight test results. The trailing edge pressure data divergence criterion underestimates the buffeting onset boundary, but the magnitude of the pressure divergence can be adjusted for better results.

1 Introduction

The buffeting onset is defined as a vibration of $\pm 0.08g$ in the pilot's seat position, usually caused by flow separation of the wing. During aircraft flight mission it is usual to maintain a maneuvering margin of 1.3g[1] in respect to the buffeting onset boundary. This operational margin can impose limitations to aircraft performance during several flight phases and should be considered since the conceptual design phase and verified during the detailed design phase[2].

Transonic buffeting onset is usually associated with the shock induced separation in the wing, and it has been studied since the airplane

reached near sound speed[3]. Gadeberg and Ziff[3] addressed a comparison of many steady aerodynamics coefficients criteria and pressure distribution to flight test results as early as 1951.

Some recent studies[4, 5] have used CFD (Computer Fluid Dynamics) to identify the buffeting boundary, but the wind tunnel is still the most used and reliable method[1]. Unsteady pressure measurements have also been used at wind tunnel testing[6] but the methodology to correlate the pressure oscillations to real flight structure vibration are complex.

Mabey[7] proposed the methodology of wing root strain gauge measurements on rigid wind tunnel models and evaluated the results with flight test data of seven aircraft. Mabey's methodology is proposed as a standard by ESDU 87012[1].

Recently, a new criterion based on wind tunnel steady aerodynamics coefficients has been satisfactorily evaluated with flight test results of four aircraft[8]. This criterion and associated methodology is used as a reference for the present work due to the lack of flight test results.

In present paper the wind tunnel data of the RMS vibration data divergence, the buffeting coefficient proposed by Mabey[7] and the trailing edge pressure divergence[1] are compared to the reference criterion for evaluation.

1.1 Wind tunnel data

The two sets of wind tunnel data used in this work are from civil jet transport aircraft that cruise in

the transonic regime. The wind tunnel tests were performed using a conventional rigid aircraft model with steel wing, flow-through nacelles¹ and tail-off configuration.

The tests were performed in pressurized wind tunnels at a Reynolds number of 3.0 million, referenced to the mean aerodynamic chord (MAC). Transition trips were used to guarantee similarity of turbulent flow of flight conditions. Steady forces and moment data were obtained by an internal balance.

A strain gauge and an accelerometer were installed in wing root and tip, respectively. This data was recorded as RMS data and is available for aircraft number 6. Steady wing pressure were measured along 10 spanwise sections of the wing, including a tap at the trailing edge (TE), and are available for aircraft number 5 and 6 (see table 1).

Table 1: Wind tunnel data

Aircraft n°	Trailing edge pressure	Strain gauge and Accelerometer
5	X	
6	X	X

2 Buffeting onset criteria

2.1 Reference criterion

Since there is no flight test results available for aircraft 5 and 6, the buffeting onset boundary based on the maximum value of second derivative of the steady moment coefficient (C_M) in respect to steady lift coefficient (C_L), named $C_M \times C_L$ criterion, is used as the reference criterion[8]. This criterion has been evaluated with flight test buffeting onset boundary within an overall standard deviation of ± 0.04 in C_L .

The buffeting onset boundary estimated by the $C_M \times C_L$ criterion extrapolated to flight test Reynolds number are compared to flight test results and presented for aircraft 1 to 4 in figures 1, 2, 3 and 4, respectively. The results are presented

¹Only in aircraft number 6.

in terms of trimmed lift coefficient² (C_{LTRIM}) and the standard deviation bar, considering all data points (± 0.04), are also present.

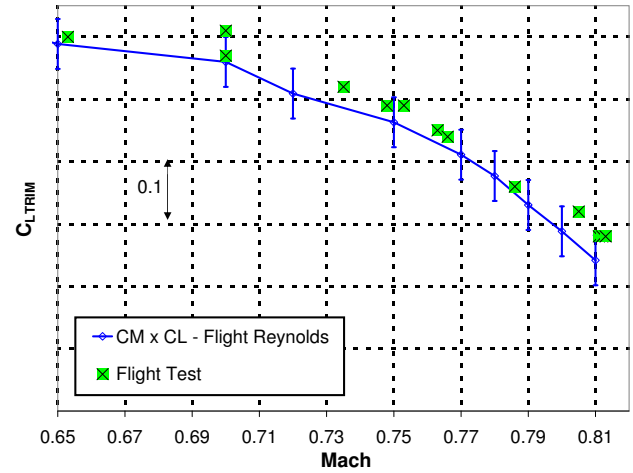


Fig. 1 : $C_M \times C_L$ criterion X Flight - Aircraft 1

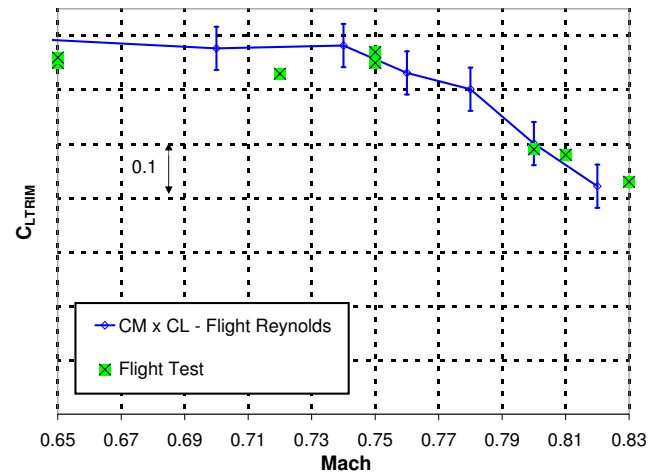


Fig. 2 : $C_M \times C_L$ criterion X Flight - Aircraft 2

2.2 Wing root strain gauge criteria

Two criteria based on the RMS data of the wing root strain gauge are evaluated. The first one is based on the divergence of the wing vibration. The second one is the buffeting coefficient, which offers a way to quantify the magnitude

²Trimmed term is used to reference the total C_L of the aircraft, including the necessary horizontal tail C_L to zero the total moment around the center of gravity.

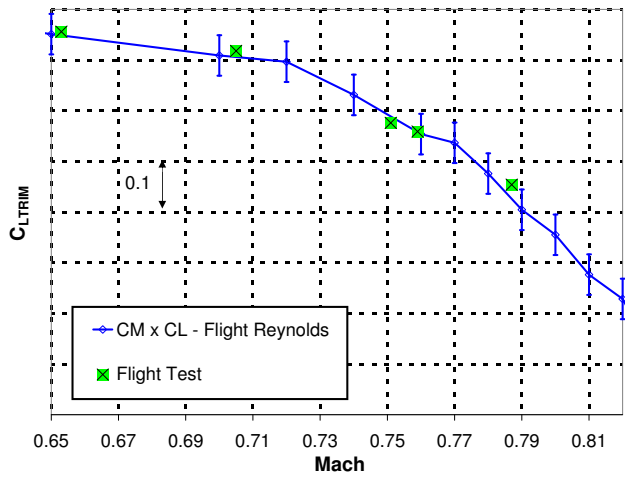


Fig. 3 : $C_M \times C_L$ criterion X Flight - Aircraft 3

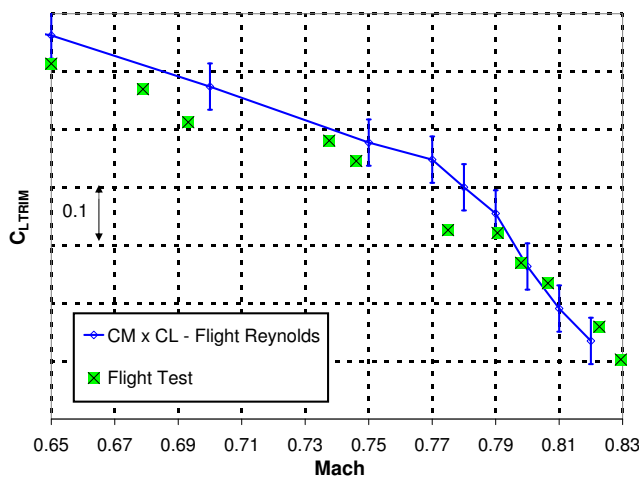


Fig. 4 : $C_M \times C_L$ criterion X Flight - Aircraft 4

of the vibration. Both criteria were proposed by Mabey[7].

The strain gauges are installed as close as possible to the wing root, near the wing upper surface of the wind tunnel model. The data is measure by high frequency equipment and the RMS value for each angle of attack (Alpha) data point is acquired. It may be used a filters around the first bending mode frequency of the wing model to isolate response that is of interest. The first bending mode frequency of the wing is measured with the same equipment but in a no wind condition.

Accelerometers installed in the wing tip can also be used with the same purpose (see figure

5). Both the strain gauge and the accelerometers are indirectly measuring the vibration of the wing, but by different variables. It is expected that the RMS results of both instruments are similar.

Although the wind tunnel model is not structurally representative of the real airplane, if the aerodynamic similarity is guaranteed, it is expected that the cause of aircraft vibration, detached flow due to shock wave separation, usually in the wing, occurs at the same condition (C_L). The magnitude of the vibration may not be similar, but it is possible to be calibrate it to match flight test results, in the case of buffeting coefficient. The present work also aims to evaluate such a comparison.

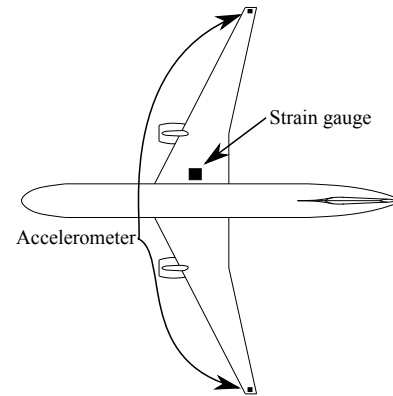


Fig. 5 : Schematic installation of strain gauge and accelerometer in the wind tunnel model

The methods based on wing vibration are a direct measurement of wing buffeting onset of the wind tunnel model, unlike the indirect estimative based on aerodynamic and pressure coefficients.

2.2.1 Wing root strain gauge divergence

The wing root strain gauge divergence criterion is defined at the angle of attack in which the vibration increases rapidly, as can be seen in figure 6.

Even at low angle of attack, in which attached flow is expected in all aircraft components, there is a baseline level of vibration. This vibration

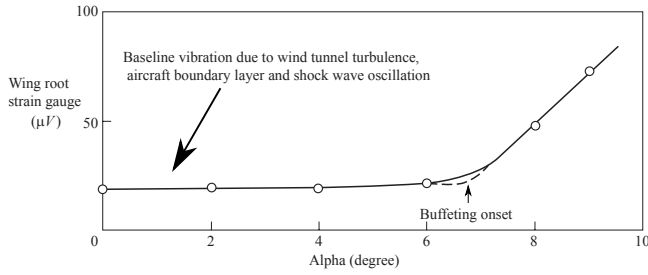


Fig. 6 : Wing root strain gauge criterion

is mainly associated with the wind tunnel turbulence level, but the turbulence in boundary layer and possibly a unsteady shock wave movement, if present, also contributes.

The RMS data of the left and right wing tip accelerometer and the right wing root strain gauge of aircraft 6 at Mach number of 0.78 is presented in figure 7 in function of alpha.

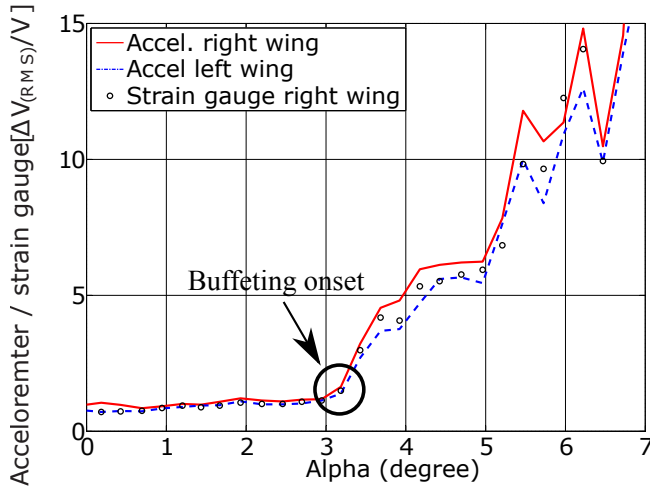


Fig. 7 : Accel. and Strain gauge - Mach 0.78 - Aircraft 6

It is possible to verify the good correspondence of accelerometers and strain gauge, defining the onset of the buffeting at the same angle of attack. Such a good correlation is verified at all Mach numbers tested. This result evaluate that both types of vibration methods can be used to obtain the same result. During the present work only the strain gauge data was used for the buffeting determination.

2.2.2 Buffeting coefficient

The dimensional buffeting coefficient (C_B) is determined by the strain gauge measured data divided by the dynamic pressure (q) and are function of the Mach number and angle of attack (equation 1).

$$C_B = \frac{\text{Strain gauge RMS signal}}{q} = C_B(\text{Mach}, \text{Alpha}) \quad (1)$$

Mabey suggests that the C_B of zero angle of attack (C_{B0}) may be used as a “tare” of the baseline vibration, in order to separate the wind tunnel induced vibration from the aircraft induced vibration. This “tare” is based on the assumption that the aircraft is not significantly contributing to the vibration at this condition (should be with the flow completely attached). For a good design airplane in operational condition this is a good assumption.

The C_{B0} is then correlated to the measured turbulence level of the wind tunnel to obtain a calibration between the excitation and the model wing response (equation 2). The turbulence level of the wind tunnel used in aircraft 6 test was not available, and it was decided to use the value of NASA Langley 7ft x 10ft (0.015)[7] for this study.

$$C_B(M, 0) = K \sqrt{nF(n)} \quad (2)$$

Where:

- $\sqrt{nF(n)}$ = wind tunnel turbulence level around the first bending mode frequency of the wing model.
- K = scaling factor between wind tunnel turbulence level and C_{B0} .

The buffeting coefficient corrected by the scaling factor is named C'_B , and obtained by equation 3.

$$C'_B(M, 0) = \frac{1}{K} C_B(M, 0) \quad (3)$$

Finally, the corrected buffeting coefficient (C''_B) is obtained using the “tare” of the zero angle

of attack vibration, by root mean square, as presented in equation 4. This the final form of the buffeting coefficient that should be related to the vibrations caused by the aircraft itself.

$$C_B''(M, \alpha) = \sqrt{CB'(M, \alpha)^2 - C_B'(M, 0)^2} \quad (4)$$

Based on a comparison of C_B'' obtained in wind tunnel to 9 aircraft flight test results, Mabe established the following levels of buffeting (see table 2). This classification is going to be used in the results analysis.

Table 2: Buffeting levels for C_B'' [7]

C_B''	Buffeting level
0.004	Weak
0.008	Moderate
0.016	Strong

The corrected buffeting coefficient (C_B'') of aircraft 6 at Mach number of 0.78 is presented as an example in figure 8. The three levels of intensity are also shown in the figure. Due to the mean square root method applied, all values are positive and are zeroed at angle of attack of zero degree.

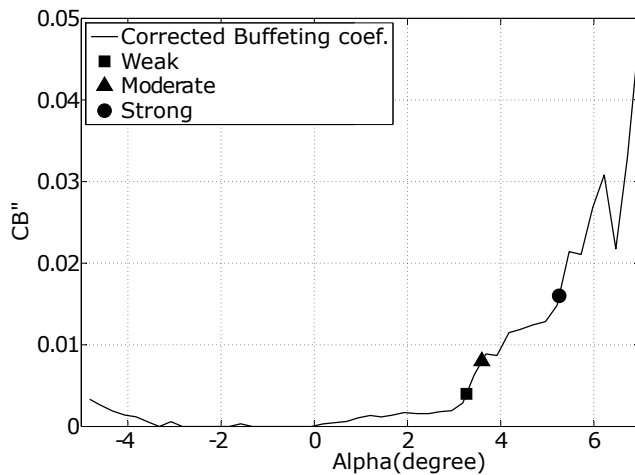


Fig. 8 : $C_B'' \times \alpha$ - Mach 0.78 - Aircraft 6

2.3 Trailing edge pressure criterion

Attacked flow usually determines a pressure coefficient (C_P) between 0.0 and 0.2 in the trailing

edge (C_{PTE}). As the angle of attack is increased the C_P usually gets more negative due to boundary layer thickening effect and suddenly diverges to significant more negative values. ESDU[1] suggests the trailing edge pressure divergence as criterion for flow detachment determination, which can be used as an indirect prediction of the onset of buffeting. Clark and Pelkman[9] presented results for the MD-11 buffeting onset estimate using the threshold of -0.04 in C_P .

In the present study wind tunnel pressure data of 10 wingspan sections are available for aircraft 5 and 6. Similar to the critical section method used for maximum lift coefficient prediction[10], the criterion will define the buffeting onset when the first wing section diverges -0.04 in C_P . The zero angle of attack is once again used as the reference "tare" value for attached C_P of each wing section.

The C_{PTE} in function of alpha along the wing span sections ($2y/b_{ref}$) are presented in figure 9 at Mach number of 0.78 for aircraft 6. Until the angle of attack of 3° the main trend is decrease in C_{PTE} value. At 3° the wing section of 75% of span diverges to negative values, indicating the flow separation at this section. The detachment is first followed by the near sections (64% and 87%) and then by the outer sections until 42% of span.

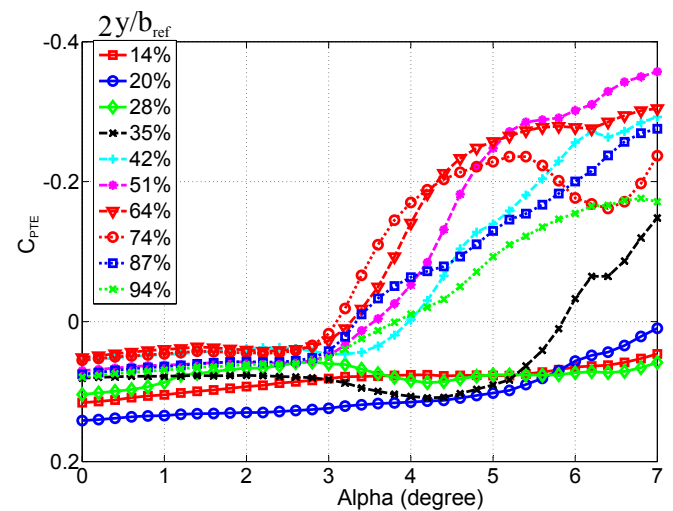


Fig. 9 : $C_{PTE} \times \alpha$ along wing span sections - Mach 0.78 - Aircraft 6

Sections 28% and 35% presents different trend after the 74% separation, increasing the C_{PTE} value. Considering the four inner sections, only 35% presents a clear pressure divergence, 2.5° after the 74% separation.

Applying the criterion to this Mach number data, a difference of -0.04 in C_{PTE} from the 0° value of each section, the buffeting onset is defined by the section at 74% of wingspan at alpha of 3° .

In figure 10 the angle of trailing edge pressure divergence of each section is presented as a function spanwise position. Another separation criterion, the most rear position of shock wave[1], is also presented for comparison.

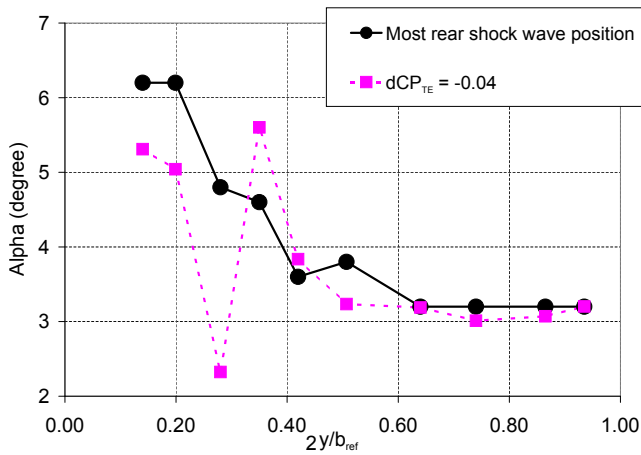


Fig. 10 : TE pressure criterion and the most rear shock wave position X wingspan - Mach 0.78 - Aircraft 6

Both criteria agree in the tip sections, and there are discrepancies in the order of one degree in the more inner sections. There is an exception in section at 28% of span. This section is located close to the pylon and nacelle of the engine, and this component is possibility contaminating the trailing edge measure, defining a very low angle of divergence. Taking a closer look at figure 9 it is possible to verify that this section decreases -0.04 in C_{PTE} in a very subtle behavior, not compatible to a flow separation.

The same C_{PTE} data along wingspan is presented in figure 11 for many Mach numbers. At Mach number of 0.70 the premature divergence of section at 28% of span does not appear. For

the higher Mach number the same behavior of figure 10 is present. This is a indication that the transonic flow around the pylon and nacelle is modifying the flow at this section. Due to this discrepancy this section is not going to be considered in the buffeting onset determination by this criterion³.

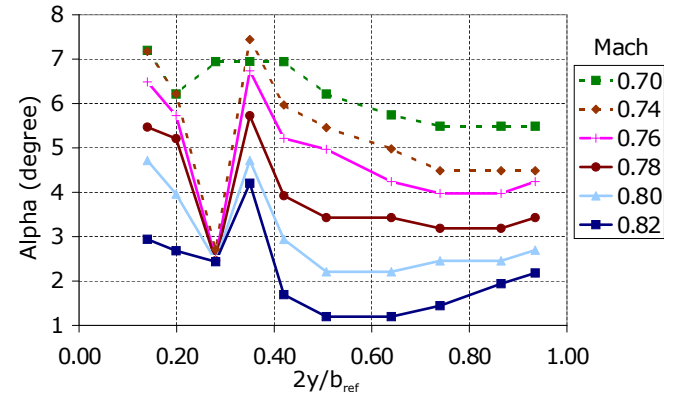


Fig. 11 : TE pressure criterion along wingspan - Many Mach numbers - Aircraft 6

3 Results

In this section the results of the buffeting onset analysis using the trailing edge pressure and strain gauge criteria for aircraft 5 and 6 wind tunnel data are evaluated with the reference criterion, the $C_M \times C_L$ criterion.

3.1 Strain gauge criterion

3.1.1 Aircraft 6

Strain gauge data is only available for aircraft number 6. The results for the strain gauge divergence criterion and the three levels of intensity of buffeting of the buffeting coefficient (C_B'') is presented in figure 12. The $C_M \times C_L$ criterion is also shown. All the data was trimmed at forward center of gravity.

At Mach 0.70 all criteria predicts the buffeting at almost the same C_{LTRIM} . The analysis of the wing pressure data at the critical section of

³Aircraft 5 does not have pylon and nacelle installed in the wing and does not have early trailing edge criterion separation as aircraft 6.

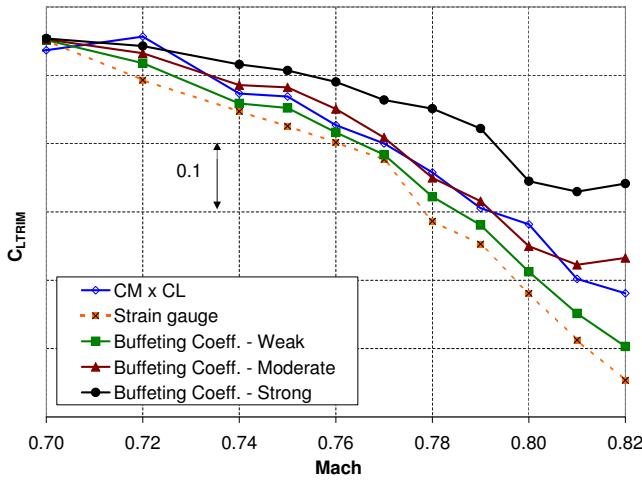


Fig. 12 : Wing root strain gauge criteria results – Aircraft 6

74% of wingspan, at the buffeting onset angle of attack, 0.5° before and also 0.5 after, figure 13, indicates an abrupt separation. This separation is caused by a high suction peak at the leading edge that results in supersonic flow and a strong shock around 25% of the section chord. This is a transonic leading edge stall. The data of other sections indicates that at this Mach number 50% of the wing separates at almost the same angle of attack.

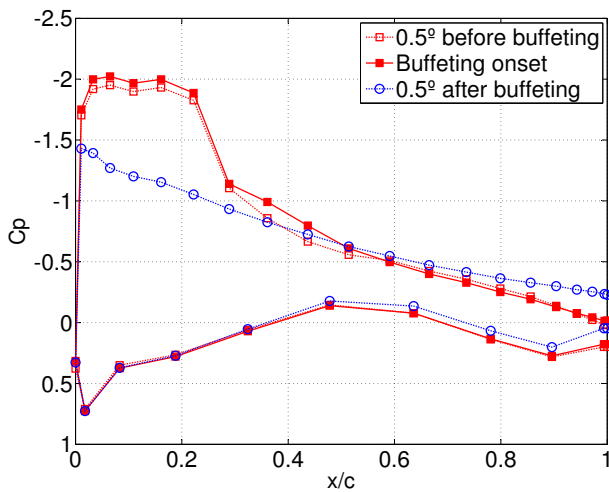


Fig. 13 : Wing section pressure distribution at 74% of wingspan - Mach 0.70 - Aircraft 6

Another data that confirms the abrupt stall characteristics is the fact that all the buffeting coefficient are together at Mach 0.70. The C_B'' as

function of angle of attack for Mach 0.70 is presented in figure 14 and the sudden increase in vibration is made clear. The sudden stall characteristic of this Mach number collapses all the criteria, leaving no margin for differences.

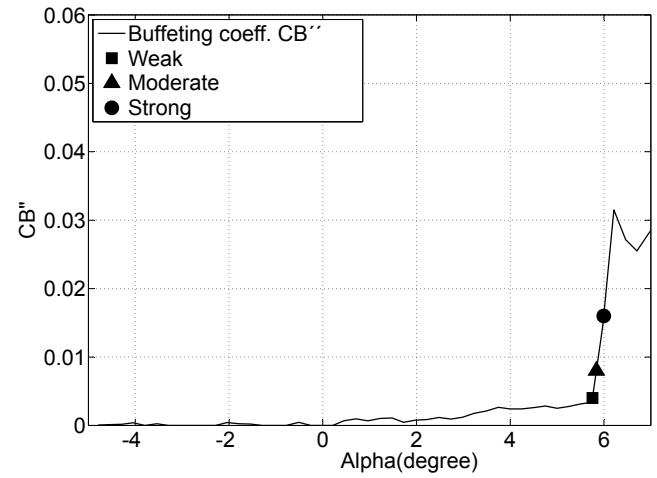


Fig. 14 : $C_B'' \times \alpha$ - Mach 0.70 - Aircraft 6

At higher Mach number the criteria spread. The leading edge suction peak gets lower and the supercritical airfoil promotes a flat supersonic region that ends in a shock further downstream as the Mach number is increased. The pressure data for Mach 0.82, section at 74%, centered in the alpha of the strain gage buffeting onset is presented in figure 15. The analysis indicates that the separation starts at the base of the shock and slowly propagates upstream with a continuous suction peak increase.

The buffeting coefficient as a function of angle of attack is presented in figure 16 for Mach number 0.82 confirming the slow development of vibration.

Analyzing figure 12, the strain gauge divergence criterion predicts a lower boundary than the $C_M \times C_L$ criterion. As concluded in the $C_M \times C_L$ criterion studies[8], the buffeting onset is actually set when a significant part of the wing is already separated. It is possible to infer that the strain gauge starts to diverge at the first sign of separation, and thus this is probably the cause of underestimation of the flight buffeting onset.

The divergence of the strain gauge is in accordance to the buffeting coefficient criteria, and set

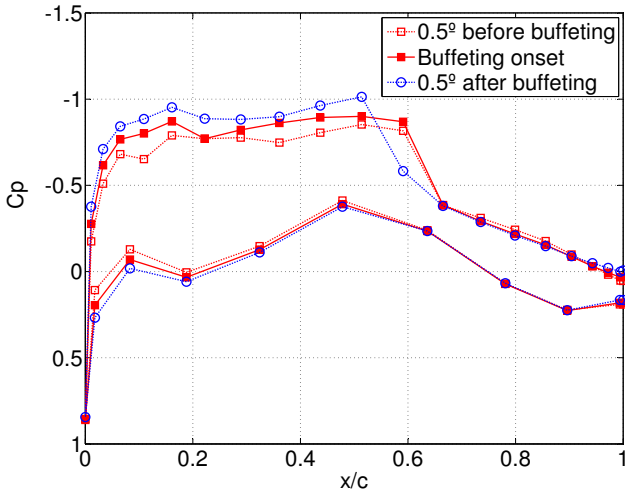


Fig. 15 : Wing section pressure distribution at 74% of wingspan - Mach 0.82 - Aircraft 6

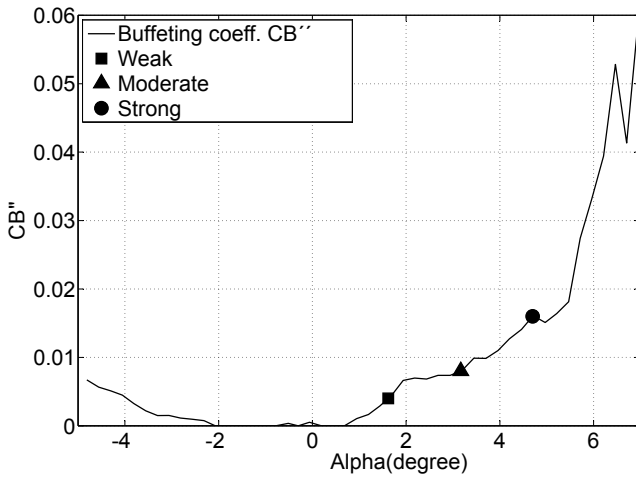


Fig. 16 : $C_B'' \times \alpha$ - Mach 0.82 - Aircraft 6

as a very weak intensity level. As the separation spreads along the chord and span the intensity of the buffeting increases and the different levels of vibration present monotonic and coherent data.

The moderate level of vibration is quite similar to $C_M \times C_L$ criterion. This similarity takes to the indirect conclusion that the level of vibration required to define the flight test buffeting onset is moderate.

3.2 Trailing edge pressure criterion

3.2.1 Aircraft 6

The results of the trailing edge criterion are compared to the $C_M \times C_L$ and straining gauge criteria at

figure 17. The pressure based criterion underestimates the boundary in respect to the other criteria at lower Mach number numbers, and presents almost identical values to the strain gauge criterion for Mach above 0.77.

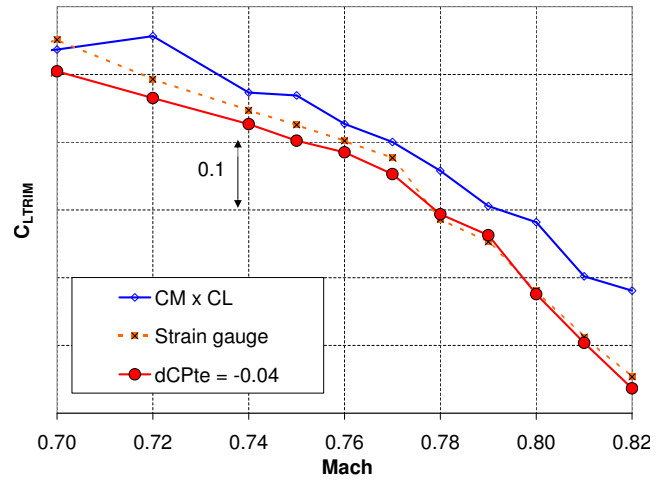


Fig. 17 : Trailing edge pressure criterion result – Aircraft 6

This results indicates that the difference of -0.04 in C_{PTE} is reasonable for the identification of flow separation, and as the strain gauge criterion, it is underestimating the buffeting onset when compared to the reference criterion.

3.2.2 Aircraft 5

The buffeting onset boundary estimated by the trailing edge criterion for aircraft 5 is compared to the reference criterion in figure 18. The relative behavior of the curves is quite similar to aircraft 6, with the ΔC_{PTE} criterion underestimating the onset of the flight buffeting along all the Mach range studied.

Both the strain gauge and ΔC_{PTE} criteria adequately predicts the start of flow separation but the buffeting onset is actually defined when part of the wing is already separated, and thus they probably underestimate the flight test buffeting onset according to the reference criterion.

The flow separation predicted by the trailing edge pressure is compared to the most rear shock wave position along the wingspan in figures 19, 20 and 21 at the Mach numbers of 0.70, 0.78 and 0.82, respectively. The correlation of the criteria

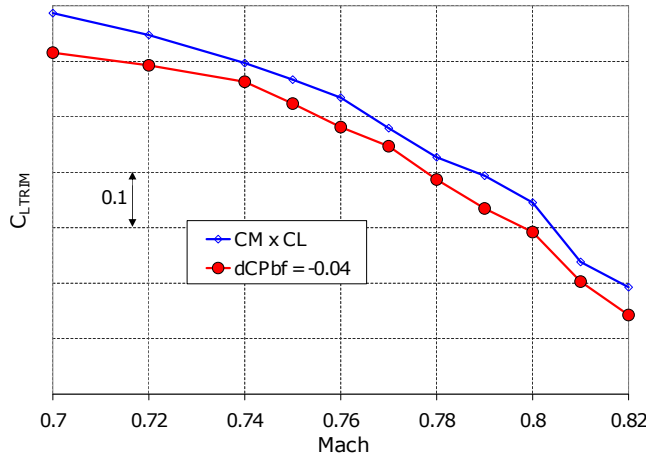


Fig. 18 : Trailing edge pressure criterion result – Aircraft 5

is reasonable, and the ΔC_{PTE} does not present the outlier value in the section around 35% as seen in aircraft 6. Aircraft 5 was tested in a wing-fuselage configuration only. The absence of the pylon and nacelle and related result is another indication that these parts promoted an alteration of pressure in the near sections at aircraft 6.

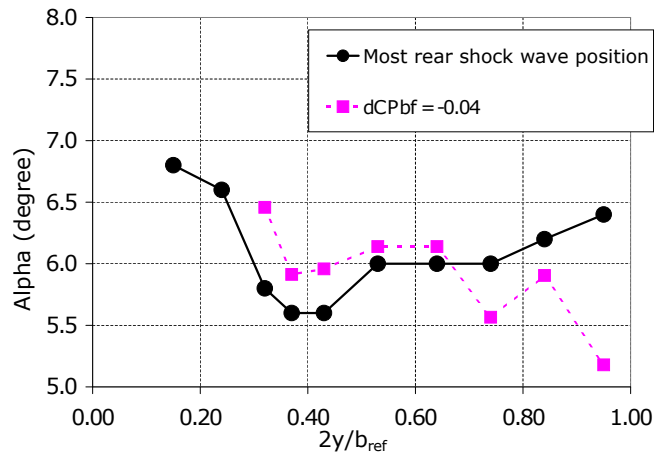


Fig. 19 : TE pressure criterion and the most rear position of shock wave along wingspan - Mach 0.70 - Aircraft 5

4 Conclusion

The transonic buffeting onset boundary estimated by trailing edge pressure divergence, wing root strain gauge divergence and the buffeting coefficient criteria was evaluated with a reference criterion, named $C_M \times C_L$. Wind tunnel data of two

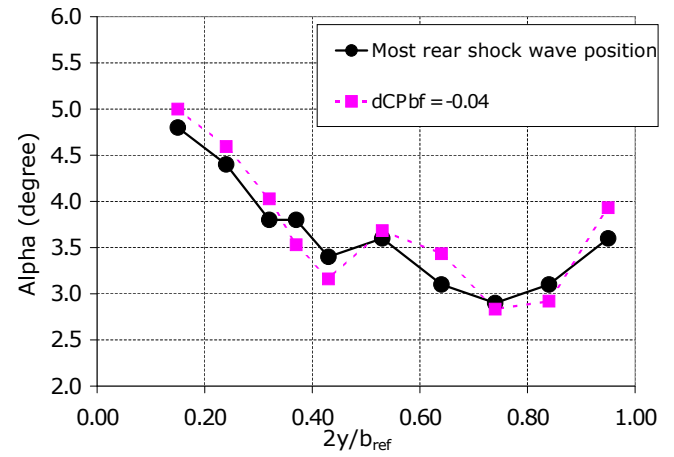


Fig. 20 : TE pressure criterion and the most rear position of shock wave along wingspan - Mach 0.78 - Aircraft 5

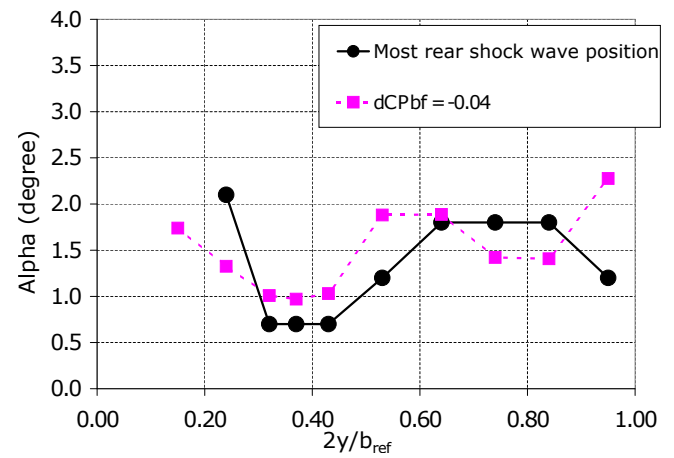


Fig. 21 : TE pressure criterion and the most rear position of shock wave along wingspan - Mach 0.82 - Aircraft 5

modern transport aircraft has been used for the study.

The results indicates that both the trailing edge pressure criterion and the strain gauge divergence criterion underestimates the flight test buffeting onset, based on the reference criterion comparison. The threshold of the pressure based criterion could be calibrated to approximate the $C_M \times C_L$ criterion. The divergence of the strain gauge criterion is not passable for calibration, but it is consistent as a very weak buffeting onset vibration level and coherent to the buffeting onset coefficient.

The work here in presented is based only on

two different aircraft, and the increase in the database would add confidence to the criteria. A calibration of the trailing edge pressure criterion may be viable and could be a interesting methodology that requires only trailing edge pressure data along the wingspan. This methodology could be used both in wind tunnel tests as flight tests, aiming to broaden the aerodynamic understanding of the aircraft.

The buffeting onset criterion shows consistency between its different levels of intensity and with the strain gauge divergence criterion. The moderate intensity buffeting approximates the reference criterion and is indicated as a procedure to predicts the flight test buffeting onset boundary. The experimental procedure and instrumentation is simple and viable to be added in any wind tunnel test with low logistics and cost impacts.

Referências

- [1] ESDU, "An introduction to aircraft buffet and buffeting", No. 87012, 1977.
- [2] Adrien Berard and Askin T. Isikveren, "Conceptual Design Prediction of the Buffet Envelope of Transport Aircraft" *Journal of Aircraft*, Vol. 46, No. 5, 2009.
- [3] Burnett L. Gadeberg and Howard L. Ziff, "Flight-determined buffet boundaries of ten airplanes and comparison with five buffeting criteria," *NACA Report*, 50i27, Washington, 1951.
- [4] David Nixon, "A Method of Estimating the onset of shock induced Buffet *AIAA Aerospace Sciences Meeting and Exhibit*, No. 0713, Reno, Nevada, 2001.
- [5] Injae Chung and Duckjoo Lee and Taekyu Reu, "Prediction of transonic Buffet onset for an airfoil with shock induced separation bubble using steady Navier-Stokes solver *AIAA Applied Aerodynamics Conference*, No. 2934, St Louis, Missouri, 2002.
- [6] B. Benoit and I. Legrain, "Buffeting Prediction for Transport Aircraft Applications Based on Unsteady Pressure Measurements", *AIAA Journal*, Vol. 87, No. 2356, Bethesda, Maryland, 1987.
- [7] D. G. Mabey, "An Hypothesis for the Prediction of Flight Penetration of Wing Buffeting from Dynamic Tests on Wind Tunnel Models", *Aeronautical research council current papers*, No. 1171, Bedford, 1971.
- [8] Sousa, Rodrigo S and Girardi, Roberto D and Annes da Silva, Roberto G, "A new criterion for transonic buffeting onset estimation", *35th AIAA Applied Aerodynamics Conference*, No. 4231, Denver, Colorado, 2017.
- [9] R.W. Clark and R.A. Pelkman, "High Reynolds Number Testing of Advanced Transport Aircraft Wings in the National Transonic Facility", *AIAA Aerospace Sciences Meeting and Exhibit*, No. 0910, AIAA, Reno, Nevada, 2001.
- [10] Wakayama, Sean and Kroo, Ilan, "Subsonic wing planform design using multidisciplinary optimization", *Journal of Aircraft*, Vol. 32, No. 4, pages 746-753, 1995.

5 Contact Author Email Address

- Rodrigo Sorbilli C. de Sousa: rodrigorsorbilli@gmail.com
- Roberto da Motta Girardi: girardi.0506@gmail.com
- Roberto Gil Annes da Silva: gil@ita.br

Copyright Statement

The authors confirm that they, and/or their company or organization, hold copyright on all of the original material included in this paper. The authors also confirm that they have obtained permission, from the copyright holder of any third party material included in this paper, to publish it as part of their paper. The authors confirm that they give permission, or have obtained permission from the copyright holder of this paper, for the publication and distribution of this paper as part of the ICAS proceedings or as individual off-prints from the proceedings.